Experimental Dermatology 2020 ;Volum 00. s. 1-13 (DOI: 10.1111/exd.14217)

Early transcriptional changes after UVB treatment in atopic dermatitis includes inverse regulation of IL-36γ and IL-37

Astrid H Lossius[1,2,3], Teresa L Berents[2], Frank Sætre[3], Hogne R Nilsen[3], Maria Bradley[4], Samina Asad[4], Guttorm Haraldsen[1,3*], Olav Sundnes[2‡], Jan-Øivind Holm[1,2‡]

[1]Institute of clinical medicine, University of Oslo, Oslo, Norway, [2]Department of Dermatology, Oslo University Hospital, Oslo, Norway, [3]Department of Pathology, Oslo University Hospital, Oslo, Norway, [4] Division of Dermatology and Venereology, Department of Medicine, Karolinska Institutet, Stockholm, Sweden

‡Shared senior authorship
*Corresponding author: Guttorm.haraldsen@medisin.uio.no, Guttorm Haraldsen, Department of Pathology, Oslo University Hospital HF, Postboks 4950 Nydalen, 0424 Oslo, Norway. Phone: (+47) 23 07 14 92 Fax: (+47) 23 07 15 11

Abstract

Background: Phototherapy with narrow-band Ultraviolet B (nb-UVB) is a major therapeutic option in atopic dermatitis (AD), yet knowledge of the early molecular responses to this treatment is lacking.

Objective: To map the early transcriptional changes in AD skin in response to nb-UVB treatment.

Methods: Adult patients (n = 16) with AD were included in the study and scored with validated scoring tools. AD skin was irradiated with local nb-UVB on day 0, 2 and 4. Skin biopsies were taken before and after treatment (day 0 and 7) and analyzed for genome-wide modulation of transcription.

Results: When examining the early response after three local UVB-treatments, gene expression analysis revealed 77 significantly modulated transcripts (30 down- and 47 up-regulated). Among them were transcripts related to the inflammatory response, melanin synthesis, keratinization and epidermal structure. Interestingly, the proinflammatory cytokine IL-36γ was reduced after treatment, while the anti-inflammatory cytokine IL-37 increased after treatment with nb-UVB. There was also a modulation of several other mediators involved in inflammation, among them defensins and S100 proteins.

Conclusion: This is the first study of early transcriptomic changes in AD skin in response to nb-UVB. We reveal robust modulation of a small group of inflammatory and anti-inflammatory targets, including the IL-1 family members IL36γ and IL-37, which is evident before any detectable changes in skin morphology or immune cell infiltrates. These findings provide important clues to the molecular mechanisms behind the treatment response and shed light on new potential treatment targets.

Keywords:

Atopic dermatitis, inflammation, microarray, UVB, keratinocytes

1 Introduction

Phototherapy with narrow-band ultraviolet B (nb-UVB) is a major therapeutic option in atopic dermatitis (AD) [1], the most common inflammatory skin disease [2-4]. It is effective in the majority of patients[5-7], but the treatment is time-consuming and often not available for practical reasons. These limitations are strong incentives to expand our knowledge and molecular understanding of UV-radiation in AD.

The mechanism of action of nb-UVB in AD is poorly understood. To date, most studies have focused on the effect of nb-UVB on immune cells. UV-light inhibits the antigen-presenting function of Langerhans cells, alters the cytokine production in the skin and induces apoptosis of infiltrating T-cells [8,9]. It has been suggested, however, that keratinocytes also play a key role in mediating the effects of nb-UVB. Keratinocytes make up the main cellular part of epidermis where nearly 90% of nb-UVB is absorbed [10]. UV-irradiation enhances the epidermal barrier function by inducing thickening of the stratum corneum [11,12], inhibits superantigen production and modulates the level of antimicrobial peptides (AMPs) [13,14]. Thus, keratinocytes could play a key role in the anti-inflammatory response associated with recovery of AD.

The gene expression profile in AD skin differs from normal skin with respect to genes related to keratinization, epidermal structure and immune pathways, and even non-lesional AD skin differs substantially from normal skin [15]. Clinical remission is evident after weeks of treatment with nb-UVB in the majority of AD patients and in line with clinical improvement, the gene expression profile in lesional AD skin is normalized [16]. However, these changes are rather a consequence of recovery and do not reveal the early events of the anti-inflammatory cascade. A more detailed knowledge of the mechanisms inducing remission may pave the way to develop more efficient and safer treatment modalities.

In this study, we wanted to define the very early transcriptional changes in AD skin in response to nb-UVB treatment. We observed after three doses of nb-UVB a significant modulation of transcripts involved in the inflammatory response, melanin-synthesis, keratinization and epidermal structure. In particular, this included an inverse modulation of the pro-inflammatory cytokine IL-36γ and the anti-inflammatory IL-37.

2 Materials and Methods

2.1 Patients

16 adult patients with AD according to the criteria of Hanifin and Rajka [17] were recruited to the study (5 males, 11 females; mean age 32, range 20-73, see Table S1 for more details). The study was approved by the Regional Ethical Committee (2017/466) and written consent was obtained from all participants.

The patients abstained from topical immunosuppressive therapy such as steroids and calcineurin inhibitors for two weeks before inclusion, and from systemic immunosuppressive therapy for at least four weeks before inclusion. The inclusion period was from October 2017 to April 2018 to minimize outdoor sun exposure. Disease severity and morbidity was assessed with validated scoring tools: SCORing Atopic Dermatits (SCORAD) [18], Eczema Area and Severity Index (EASI) [19], Patient-Oriented Eczema Measure (POEM) [20], and Dermatology Life Quality Index (DLQI) [21]. Saliva samples were genotyped for the three most common mutations in the gene encoding filaggrin; R501X, R2447X and 2282del4. Genotyping was done with Taqman primer/probe assays from ABI according to manufacturer's protocol. Blood serum samples were taken to measure IgE and eosinophils.

2.2 Nb-UVB treatment:

The minimal erythema dose (MED), defined as the barely detectable erythemal dose of nb-UVB [22], was established with the Dermalight® 80 MED-tester (Dr Hönle Medizintechnik). One lesion with active AD was irradiated with 1 MED with the small hand-held nb-UVB device Dermalight®80 (Dr Hönle Medizintechnik) every 48H (on day 0, 2 and 4). Subsequently the patients underwent standard full-body nb-UVB treatment three times per week for 6-8 weeks (in total 12-25 sessions) with a starting dose of 0.1-0.2 J/cm^2 and gradual

increments in dose, see Table S2 for UVB dosages and Figure 1A for experimental design (illustrations from: https://smart.servier.com).

2.3 Skin biopsies:

Punch biopsies of 4 mm were taken from the lesion with active AD before irradiation, after three local treatments with nb-UVB (day 7) and after 6-8 weeks of full-body nb-UVB treatment. The biopsies were taken within the same eczematous lesion, but more than 1 cm from the previous scar. Non-lesional sun-protected skin (nates) was also biopsied, prior to and after full body nb-UVB treatment. The biopsies were immediately bisected: one half was preserved in RNAlater and kept at -70°C for RNA isolation, the other half was fixed in formalin and embedded in paraffin.

2.4 RNA isolation:

RNA was purified with the RNeasy Mini Kit (Qiagen), including digestion with Proteinase K (Qiagen). Tissue samples were solubilized with the MP FastPrep 24 homogenizer using fast prep tubes containing Lysing Matrix D ceramic spheres (MP Biomedicals). All samples were treated with DNAse to remove genomic DNA (RNase-Free DNase Set, Qiagen) before measuring RNA concentrations with NanoDrop 2000 (ThermoFisher) and RNA-quality with the Agilent 2100 Bioanalyzer using the Agilent RNA 6000 Nano kit (Agilent Technologies). Samples with a RIN (RNA integrity number) value > 7.5 were accepted for further analysis.

2.5 Quantitative RT-PCR (qRT-PCR):

Total RNA was reverse transcribed using SuperScript III Reverse Transcriptase cDNA system (Thermo Scientific™), oligo (dT) primers, and dNTPs (GE Healthcare). Quantitative RT-PCR (qRT-PCR) was carried out with an AriaMx Real Time PCR System instrument and analyzed by Agilent Technologies AriaMx software (Agilent Technologies). Transcript levels of *IL37*

and *IL36γ* were normalized against transcript levels of *hprt* and the relative gene expression levels were calculated using the delta Ct method [23].

Primers: IL-37 fw: GGA CAA AGT CAT CCA TCC CTT C rv: GAG CCC ACC TGA GCC CTA TAA; IL-36γ fw: GCC CAC ATT GCA GCT AAA AG rv: AGG AGG CAA TGA ACC AGT CC.

2.6 Immunostainings

Formalin-fixed, paraffin-embedded (FFPE) tissue sections (4 µm thick) were deparaffinized before heat-induced epitope retrieval by boiling in buffer (Tris pH 9 target retrieval buffer or Target Retrieval Solution pH 6; DAKO) for 20 minutes. Blocking was performed by incubation in 5% serum from the host of the secondary antibody for 30 minutes at RT, followed by incubation with the primary antibodies diluted in PBS with 1.25% BSA 1.5 hours in RT or overnight at 4°C and subsequent incubation with fluorescently labelled secondary antibodies (90 min, RT). Hoechst 33248 (Sigma-Aldrich) nuclear dye (0.5 µg/mL) was used as counterstain. Cover slips were mounted in ProLong Diamond Antifade (Thermo Scientific™). Irrelevant, concentration-matched primary antibodies were used as negative controls. Keratin 16, CD3, CD4, CD8, FoxP3, Langerin, CD11c and IL-33 were detected using the automated Ventana Discovery Ultra system and DAB, Purple, Teal or Yellow HRP-responsive chromogens, all from Ventana Systems.

2.7 Image acquisition and analysis

The immunoenzymatically stained slides were scanned in a Pannoramic Midi slide scanner (3DHISTEC) and images were analyzed in the open source software QuPath version 0.2.0-m7 [24]. Dermis and epidermis were semi-automatically outlined providing measurements of the areas analyzed, and cells were counted manually in the freely available software FIJI (ImageJ) [25]. Images were obtained using an Olympus BX51 microscope with an Olympus U-

TVO.5XC camera and the AnalySIS 3.2 software (Soft Imaging systems). The images of the immunofluorescently stained slides were all acquired the same day using identical settings with a Nikon Ellipse E800 widefield microscope with Zen software (Carl Zeiss Microscopy). Images were processed and analyzed using FIJI to manually select the epidermis [25] and CellProfiler version 3.1.8 [26] to select individual cells and measure mean intensity of IL-36γ in the cytosol. Output data were organized using a customized R-based script (RStudio Team 2016, "http://www.rstudio.com/").

2.8 Antibodies

The antibodies used in this study included: mouse anti-IL-36g (ab156783, Abcam), goat anti-mouse Alexa fluor 488 (A21121, Life technologies), donkey anti-rabbit-Alexa fluor 488 (A21206, Life technologies), rabbit anti-CD3 (A0452, DAKO), mouse anti-FoxP3 (ab20034, Abcam), mouse anti-CD11c (clone 5D11, 563-L Leica Biosystems), rabbit anti-Langerin/CD207 (ab192027, Abcam), rabbit anti-Keratin 16 (ab76416, Abcam), mouse anti-CD8 (clone 4B11, MA180231, Thermo Scientific), rabbit anti-CD4 (clone SP35, MA139582, Thermo Scientific), rabbit anti-IL-37 (AG-25A-0111, Adipogen), rabbit anti-IL-37 (HPA054371, Sigma-Aldrich), rabbit anti-IL-37 (153889, Abcam)

2.9 Gene expression profiles

Gene expression profiles were performed by the Bioinformatics and Expression Analysis (BEA) core facility at Karolinska Institutet (Huddinge, Sweden) using the Affymetrix Clariom S Array. The raw data (CEL files) were imported into the freely available software Transcriptome Analysis Console (TAC, v4.0.1, Applied Biosystems, Thermo Fisher Scientific). Normalization was performed by the signal space transformation – robust multi-array average (SST-RMA) approach. In total, 21448 genes were analyzed, and differentially expressed genes were

identified by using paired analysis. Filter criteria were fold change > 2 or < -2 and the false discovery rate-adjusted p-value < 0.05. Raw data are deposited in the Gene Expression Omnibus repository (GSE150797). Gene Ontology analysis [27] was performed using the GO Consortium database (version released, 20200324) and the Panther overrepresentation test (version released, Released 20200407) [28].

2.10 Statistical analyses

Statistical analyses were performed in GraphPad Prism (version 8.0). For variables that were normally distributed the differences between the three timepoints were analyzed with repeated measures ANOVA. If this test was significant, the different timepoints were compared two by two with paired Student's t-test. For variables that were not normally distributed the differences between timepoints were tested with Friedman's test. If the test was significant, the Wilcoxon matched pairs signed rank test was used to test differences between timepoints two by two. All tests were two-sided and p-values less than 0.05 were considered statistically significant.

3 Results

All patients (n = 16) were irradiated with local nb-UVB three times before starting treatment with full body nb-UVB three times per week (see Figure 1A for experimental design). Treatment was efficient after 6-8 weeks, both according to the objective scoring tools SCORAD and EASI, and the subjective scoring tools POEM and DLQI (Figure 1B-E). Four patients had mutations in the gene encoding filaggrin, three of them being heterozygous bearers of one R501X allele, while one of them was a compound heterozygote bearing two different mutated alleles (R501X and R2447X). None of the patients had a mutation in the 2282del4 allele.

We first performed immunohistochemistry to assess whether early effects of nb-UVB were reflected in a change of epidermal hyperplasia and immune cell infiltrates. H&E-stained sections showed no changes in lesional AD skin regarding epidermal thickness after three rounds of nb-UVB treatment (Figure 2A, B) but revealed reduced epidermal thickness after 6-8 weeks of treatment (Figure 2C). Keratin 16 showed strong expression throughout all epidermal layers before treatment (Figure 2D) and remained unchanged after three local treatments of nb-UVB (Figure 2E). After 6-8 weeks of full-body treatment Keratin 16 approached the level of expression in non-lesional AD skin confining to the basal epidermal layer only (Figure 2F and data not shown). We also stained for several inflammatory cell types: T-cells ($CD3^+$) with subsets ($CD4^+$, $CD8^+$), T-regulatory cells ($FoxP3^+$), Langerhans cells ($Langerin^+$) and dendritic cells ($CD11c^+$). None of these cellular subsets were reduced by three rounds of local nb-UVB but after 6-8 weeks of treatment we observed a reduction in the number of $CD4^+$, $CD8^+$ and $CD11c^+$ cells (Figure 2G-R, Figure S1A-F). We did not observe any significant increase in the number of T-regulatory cells, and the $FoxP3/CD4^+$ ratio was unchanged (Figure S1E, F).

We next assessed the transcriptional profile of our biopsies, finding that full body nb-UVB treatment for 6-8 weeks normalized the gene expression in skin with AD (n = 14) (Figure 3A). When comparing untreated lesional and non-lesional skin, there were 696 differentially expressed genes (DEGs); 308 genes were upregulated in lesional skin compared to non-lesional while 388 genes were downregulated. When comparing lesional skin before and after full body treatment we found 442 DEGs; 195 upregulated and 247 downregulated genes. Treated lesional skin approximated non-lesional skin as we observed only one DEG after treatment (Figure 3A). A principal component analysis (PCA) of all transcripts from samples taken from the same body site before treatment, after three treatments and after 6-8 weeks of treatment showed samples to cluster in three quite distinct groups (Figure 3B, Figure S2). Subsequently we analyzed the earliest response to nb-UVB treatment, finding 77 DEGs after only three treatments of local nb-UVB: 30 down-regulated and 47 up-regulated genes (n = 16) (Figure 3A, Table 1).

We explored the functions of the DEGs after local nb-UVB by curating each hit individually and by gene ontology analysis. As expected, many of the upregulated DEGs are related to melanin synthesis (*CTSK, DCT, KIT, KITLG, MLANA, PLXNC1, PMEL, PTPRM, TYR, TYRP1* and *TRPM1*) or involved in keratinization and epidermal structure (*CTSK, EREG, FLG2, FMN1*, *KRT15*/Keratin 15, *LCE1A, LCE1B, LCE1D, LOR, PLP1, TMEM99*, *TXNIP and VIM*). However, several of the upregulated genes also have confirmed or putative roles in inflammation (*A2M, AZGP1, C5orf46, CLU, CTSH, CTSK, ENPP2, FCGR3B, FLG2, FTL, IGFBP7, IL37, KIT, KITLG/SCF, LP1, MMP2,MXRA5, PLP1, PLXNC1, SPARCL1, SERPINB12, TMEM99,TXNIP and VIM*) (Figure 3C-E). The downregulated DEGs were related to inflammation (*DEFB4A, DEFB4B, DEFB103A, DEFB103B, ENDOU, EREG, FOSL1, HEPHL1, IL36G, IL36A, ODC1, PLA2G2F, PRSS3, S100A7A and S100A12*) and keratinization/epidermal structure (*FGFBP1, LCE3A, SPRR2A, SPRR2B, SPRR2D, SPRR2F)*.

There were also differentially expressed genes with unknown function or unclear relevance (Table 1, Table S3 and Figure 3C-E).

Although a large proportion of DEGs were potentially related to inflammation, few of them were established inflammatory mediators. *IL36G* and *IL37*, members of the interleukin-1-family, were two of only a handful cytokines that appeared in our analysis. These cytokines have previously shown up in several transcriptomic analyses of AD skin [29-31]. *IL36G* and *IL37* were not only differentially expressed after three local treatments, but this change was further increased after 6-8 weeks of treatment with full-body UVB (supplementary Figure 3A, B). This suggests that these cytokines are involved in a continuous process initiated by the UVB treatment. Thus, we chose to focus our further analyses on these two highly interesting candidates

Quantitative RT-PCR analyses confirmed the downregulation of *IL36G* (Figure 4A) and the upregulation of *IL37* (Figure 4B) in response to three treatments of nb-UVB. We also wanted to confirm our results at the protein level using immunohistochemistry. We found the signal for IL-36γ limited to keratinocytes and observed a reduced signal for IL-36γ after treatment with nb-UVB after only three treatments (Figure 4C-E, Figure S4), in good agreement with our observation at the transcript level. By contrast, we assessed the suitability of three different antibodies to IL-37, but we were not able to detect any difference between timepoints with immunohistochemistry for this protein (data not shown).

4 Discussion

In this study we show that as few as three treatments of local nb-UVB modulated several transcripts of relevance to immunoregulation. In particular, we observed a reduction of inflammatory IL-36γ and an upregulation of the anti-inflammatory cytokine IL-37 in AD skin. This change in gene expression profile appeared before any effect of treatment was evident clinically or histologically, and it represents the first transcription profile induced by short course local nb-UVB in atopic eczema. A dose of 1 MED induces a slight erythema reflecting some degree of inflammation, however, we observed no signs of increased inflammation in the skin biopsies after irradiation, neither at the level of transcripts nor in terms of leukocyte recruitment. This could be explained by the timing of the second biopsy which was taken three full days (day 7) after the last dose of erythematous nb-UVB. The intra-patient approach, also used by others [32,33], reduces the variability and is likely to enhance the sensitivity of our analyses.

Nb-UVB only penetrates down to the lower part of the epidermis. Although the exact mechanisms that confer the effect on nb-UVB in atopic dermatitis are unknown, it is likely that it involves a direct effect on keratinocytes. IL-36γ was predominantly expressed in keratinocytes and this expression was rapidly reduced upon only 3 rounds of local nb-UVB. IL-36 γ is known to be predominantly expressed by epithelial cells [34] and is likely an important pro-inflammatory cytokine [35,36]. It stimulates maturation and function of dendritic cells, thereby driving T cell proliferation [34] and it is reportedly upregulated in other inflammatory skin diseases such as psoriasis [37-41] and hidradenitis suppurativa [42]. Moreover, expression of IL-36γ in keratinocytes is induced by scratching in an *in vitro* Koebner model[43]. Recent studies suggest that IL-36γ could be important in the pathogenesis of AD as IL-36γ was found highly expressed in keratinocytes, especially in the upper epidermal layers [44], and IL-36γ is elevated in acute AD, and further increased in chronic eczematous lesions

[31]. A biological drug against IL-36γ has already been tested in pustular psoriasis with promising results [45].

IL-37, another member of the IL1-family of cytokines, was one of the genes that were upregulated several folds after only three rounds of nb-UVB-therapy. There are five isoforms of IL-37[46] and the primers we used for qt-PCR was designed in order to detect all of these. Others have reported that IL-37 is expressed by epithelial cells [47] but we were unable to confirm any change in the expression of IL-37 protein by immunohistochemistry, in spite of the use of three different antibodies. A mismatch between isoforms present in the skin and the isoforms detected by the antibodies is one possible explanation. As far as we are aware of, isoform specific antibodies validated for immunohistochemistry are not commercially available. IL-37 is believed to be a strong inhibitor of innate immunity [46,48-50]and it has been shown to downregulate and silence inflammatory processes in monocytes and other cells *in vitro* [50]. Nevertheless, little is known about the role of IL-37 in skin inflammation. As IL-37 is not expressed in the mouse, few mechanistic studies have been performed to elucidate its function, yet a recent study in transgenic mice expressing either human IL-37 or mutant IL-37 deficient in nuclear sorting show that IL-37 is an anti-inflammatory cytokine whether in the nucleus or outside the cell, shedding interesting light on the nuclear and non-nuclear properties of this cytokine[48].

Supporting our findings, a recent study showed that crisaborole, a phosphodiesterase-4 inhibitor used for topical treatment of mild-to-moderate atopic dermatitis, induced the expression of IL-37 in atopic skin after only 8 days of treatment [33]. IL-37 stood out as consistently up-regulated in non-lesional AD skin compared to lesional skin in a study identifying up- and downregulated genes across five different datasets in AD [29]. Moreover, a meta-analysis combining 4 published AD datasets to define a robust disease profile for AD confirmed this behavior for IL-37 [30]. Both crisaborole and nb-UVB altered the expression of

SA100A12 and DEFB4B but in addition, crisaborole also changed the expression of several other genes were not differentially expressed in our study: *IL13, CCL17, CCL18, CCL22, IL8, IL17A, IL17F, IL23p19* and *IL31* [33]. An explanation to this discrepancy could be the different modes of action. Topical crisaborole likely penetrates beyond the epidermal compartment and directly affects intracellular signaling in most cell types including dermal immune cells, while nb-UVB primarily affects keratinocytes and other cells of the epidermal compartment. Future studies should examine early transcriptome changes in response to other AD therapeutics in order to gain more insights into the early unifying events of AD improvement.

The antimicrobial peptides, the β-defensins (*DEFB4A, DEFB4B, DEFB103A and DEFB103B)* and the S100 proteins (*S100A7A and S100A12)* are all downregulated in our study in response to nb-UVB. Downregulation of β-defensins after treatment with UVB is previously reported by Gamblicher et al who described how overexpression of human β-defensins 2 in AD was normalized after 6 weeks of nb-UVB treatment, and concomitantly levels of the constitutively expressed human defensin 1 increased [13]. However, in healthy skin β-defensins 2, 3 and S100A7 are upregulated after short-term treatment of nb-UVB (1 MED on three consecutive days [51], and both S100A7 and S100A12 were upregulated 24 hours after an erythemogenic dose of nb-UVB [52].

Other elements of our transcriptional analysis deserve mention; we found upregulation of insulin-like growth factor binding protein-7 (IGFBP7) in response to early UVB treatment. Interestingly IGFBP7 is downregulated in psoriasis and, given as a recombinant molecule, it attenuates experimental arthritis [53]. Plexin C1 (PLXNC1), an endogenous receptor of the neuronal guidance protein semaphorin 7, is also upregulated in response to UV treatment. PLXNC1 has been found to promote the acute inflammation of peritonitis [54] and it will be interesting to see whether it has other, related functions in the resolution of inflammation induced by UV-treatment. Matrix metalloproteinase 2 (MMP2) is upregulated in cutaneous

lupus erythematosus and levels correlates with disease severity [55]. Cathepsin K (CTSK) prevents inflammation and bone erosion in rheumatoid arthritis and in periodontitis [56] and ornithine decarboxylase (ODC1) is involved in attenuating the inflammatory response upon stimulation of macrophages [57]. Due to a limited amount of patient material we were not able to verify all interesting candidates with qt-PCR and immunohistochemistry.

Despite the recent development of new treatment modalities for patients with AD, there are still major gaps in our knowledge of AD pathogenesis and mechanisms leading to treatment responses. In this study we show for the first time early transcriptional changes in response to local nb-UVB. We reveal a robust modulation of a small group of immune-related genes, including the IL1-family members IL-36γ and IL-37, after only three treatments and before any changes in skin morphology or immune cell infiltrates. These findings provide important clues to the molecular mechanisms behind the treatment response, and unravel new potential treatment targets in AD.

Acknowledgements:

We would like to thank the patients who participated in this study. We would also like to thank Denis Khnykhin for valuable advice regarding the manuscript, Kjersti Thorvaldsen Hagen and Linda I. Solfjell for excellent laboratory assistance, Manuela Zucknick and the Oslo Centre for Biostatistics and Epidemiology Statistical advising Service (https://www.med.uio.no/imb/english/research/centres/ocbe/advising/) for help and advice regarding the statistical analysis, Halfdan Vier Simensen at Aviva for providing skin tissue, Aase Hoeviskeland for help in recruiting participants, IMM for analysis of serum samples and the core facility at Novum, BEA, Bioinformatics and Expression Analysis, which is supported by the board of research at the Karolinska Institute and the research committee at the Karolinska hospital for the gene expression analysis. We are also grateful to the Psoriasis and Eczema Foundation (PEF), the Norwegian Asthma and Allergy Association (NAAF)), Arne E. Ingel's endowment and Sanofi for financial support.

Conflict of Interest Statement

AHL has received unrestricted research grants from Sanofi.

Author contribution

AHL, JOH, OS, GH and TLB designed the study and analyzed and interpreted the data. AHL performed the clinical assessment and laboratory work and drafted the manuscript. AHL and HRN performed the IHC and FS and AHL analyzed the IHC stainings. SA and MB performed the genetic analyses. All authors contributed significantly, and all have read and approved the final manuscript.

References

[1] A. Wollenberg, S. Barbarot, T. Bieber, S. Christen-Zaech, M. Deleuran, A. Fink-Wagner, U. Gieler, G. Girolomoni, S. Lau, A. Muraro, M. Czarnecka-Operacz, T. Schafer, P. Schmid-Grendelmeier, D. Simon, Z. Szalai, J. C. Szepietowski, A. Taieb, A. Torrelo, T. Werfel, J. Ring. *J Eur Acad Dermatol Venereol.* **2018**, *32*, 850.

[2] T. Bieber. *Ann Dermatol.* **2010**, *22*, 125.

[3] S. Weidinger, L. A. Beck, T. Bieber, K. Kabashima, A. D. Irvine. *Nat Rev Dis Primers.* **2018**, *4*, 1.

[4] I. A. Deckers, S. McLean, S. Linssen, M. Mommers, C. P. van Schayck, A. Sheikh. *PLoS One.* **2012**, *7*, e39803.

[5] T. Gambichler. *Arch Dermatol Res.* **2009**, *301*, 197.

[6] F. M. Garritsen, M. W. Brouwer, J. Limpens, P. I. Spuls. *Br J Dermatol.* **2014**, *170*, 501.

[7] L. Vakeva, S. Niemela, M. Lauha, R. Pasternack, A. Hannuksela-Svahn, A. Hjerppe, A. Joensuu, M. Soronen, L. Ylianttila, R. Pastila, H. Kautiainen, E. Snellman, M. Gronroos, T. Karppinen. *Photodermatol Photoimmunol Photomed.* **2019**, *35*, 332.

[8] F. Breuckmann, G. von Kobyletzki, A. Avermaete, M. Radenhausen, S. Hoxtermann, C. Pieck, P. Schoneborn, T. Gambichler, M. Freitag, K. Hoffmann, P. Altmeyer. *J Eur Acad Dermatol Venereol.* **2003**, *17*, 418.

[9] J. Krutmann, A. Morita. *J Investig Dermatol Symp Proc.* **1999**, *4*, 70.

[10] J. D'Orazio, S. Jarrett, A. Amaro-Ortiz, T. Scott. *Int J Mol Sci.* **2013**, *14*, 12222.

[11] J. Jekler, O. Larko. *J Am Acad Dermatol.* **1990**, *22*, 49.

[12] A. Patrizi, B. Raone, G. M. Ravaioli. *Adv Exp Med Biol.* **2017**, *996*, 319.

[13] T. Gambichler, M. Skrygan, N. S. Tomi, P. Altmeyer, A. Kreuter. *Br J Dermatol.* **2006**, *155*, 1275.

[14] S. P. Hong, M. J. Kim, M. Y. Jung, H. Jeon, J. Goo, S. K. Ahn, S. H. Lee, P. M. Elias, E. H. Choi. *J Invest Dermatol.* **2008**, *128*, 2880.

[15] M. Suarez-Farinas, S. J. Tintle, A. Shemer, A. Chiricozzi, K. Nograles, I. Cardinale, S. Duan, A. M. Bowcock, J. G. Krueger, E. Guttman-Yassky. *J Allergy Clin Immunol.* **2011**, *127*, 954.

[16] S. Tintle, A. Shemer, M. Suarez-Farinas, H. Fujita, P. Gilleaudeau, M. Sullivan-Whalen, L. Johnson-Huang, A. Chiricozzi, I. Cardinale, S. Duan, A. Bowcock, J. G. Krueger, E. Guttman-Yassky. *J Allergy Clin Immunol.* **2011**, *128*, 583.

[17] J. M. Hanifin. *Acta Derm Venereol (Suppl).* **1980**, *92*, 44.
[18] B. Kunz, A. P. Oranje, L. Labreze, J. F. Stalder, J. Ring, A. Taieb. *Dermatology.* **1997**, *195*, 10.
[19] J. M. Hanifin, M. Thurston, M. Omoto, R. Cherill, S. J. Tofte, M. Graeber. *Exp Dermatol.* **2001**, *10*, 11.
[20] C. R. Charman, A. J. Venn, H. C. Williams. *Arch Dermatol.* **2004**, *140*, 1513.
[21] A. Y. Finlay, G. K. Khan. *Clin Exp Dermatol.* **1994**, *19*, 210.
[22] P. M. Gordon, P. J. Saunders, B. L. Diffey, P. M. Farr. *Br J Dermatol.* **1998**, *139*, 811.
[23] T. D. Schmittgen, K. J. Livak. *Nat Protoc.* **2008**, *3*, 1101.
[24] P. Bankhead, M. B. Loughrey, J. A. Fernández, Y. Dombrowski, D. G. McArt, P. D. Dunne, S. McQuaid, R. T. Gray, L. J. Murray, H. G. Coleman, J. A. James, M. Salto-Tellez, P. W. Hamilton. *Sci Rep.* **2017**, *7*, 16878.
[25] J. Schindelin, I. Arganda-Carreras, E. Frise, V. Kaynig, M. Longair, T. Pietzsch, S. Preibisch, C. Rueden, S. Saalfeld, B. Schmid, J. Y. Tinevez, D. J. White, V. Hartenstein, K. Eliceiri, P. Tomancak, A. Cardona. *Nat Methods.* **2012**, *9*, 676.
[26] A. E. Carpenter, T. R. Jones, M. R. Lamprecht, C. Clarke, I. H. Kang, O. Friman, D. A. Guertin, J. H. Chang, R. A. Lindquist, J. Moffat, P. Golland, D. M. Sabatini. *Genome Biol.* **2006**, *7*, R100.
[27] M. Ashburner, C. A. Ball, J. A. Blake, D. Botstein, H. Butler, J. M. Cherry, A. P. Davis, K. Dolinski, S. S. Dwight, J. T. Eppig, M. A. Harris, D. P. Hill, L. Issel-Tarver, A. Kasarskis, S. Lewis, J. C. Matese, J. E. Richardson, M. Ringwald, G. M. Rubin, G. Sherlock. *Nat Genet.* **2000**, *25*, 25.
[28] H. Mi, A. Muruganujan, X. Huang, D. Ebert, C. Mills, X. Guo, P. D. Thomas. *Nature Protocols.* **2019**, *14*, 703.
[29] D. Ghosh, L. Ding, U. Sivaprasad, E. Geh, J. Biagini Myers, J. A. Bernstein, G. K. Khurana Hershey, T. B. Mersha. *PLoS One.* **2015**, *10*, e0144316.
[30] D. A. Ewald, D. Malajian, J. G. Krueger, C. T. Workman, T. Wang, S. Tian, T. Litman, E. Guttman-Yassky, M. Suarez-Farinas. *BMC Med Genomics.* **2015**, *8*, 60.
[31] L. C. Tsoi, E. Rodriguez, D. Stolzl, U. Wehkamp, J. Sun, S. Gerdes, M. K. Sarkar, M. Hubenthal, C. Zeng, R. Uppala, X. Xing, F. Thielking, A. C. Billi, W. R. Swindell, A. Shefler, J. Chen, M. T. Patrick, P. W. Harms, J. M. Kahlenberg, B. E. Perez White, E. Maverakis, J. E. Gudjonsson, S. Weidinger. *J Allergy Clin Immunol.* **2019**.
[32] E. Guttman-Yassky, B. Ungar, K. Malik, D. Dickstein, M. Suprun, Y. D. Estrada, H. Xu, X. Peng, M. Oliva, D. Todd, T. Labuda, M. Suarez-Farinas, R. Bissonnette. *J Allergy Clin Immunol.* **2017**, *140*, 1032.
[33] R. Bissonnette, A. B. Pavel, A. Diaz, J. L. Werth, C. Zang, I. Vranic, V. S. Purohit, M. A. Zielinski, B. Vlahos, Y. D. Estrada, E. Saint-Cyr Proulx, W. C. Ports, E. Guttman-Yassky. *J Allergy Clin Immunol.* **2019**, *144*, 1274.
[34] A. M. Foster, J. Baliwag, C. S. Chen, A. M. Guzman, S. W. Stoll, J. E. Gudjonsson, N. L. Ward, A. Johnston. *J Immunol.* **2014**, *192*, 6053.
[35] E. Y. Bassoy, J. E. Towne, C. Gabay. *Immunol Rev.* **2018**, *281*, 169.
[36] L. Ding, X. Wang, X. Hong, L. Lu, D. Liu. *Oncotarget.* **2018**, *9*, 2895.
[37] C. Bridgewood, G. W. Fearnley, A. Berekmeri, P. Laws, T. Macleod, S. Ponnambalam, M. Stacey, A. Graham, M. Wittmann. *Front Immunol.* **2018**, *9*, 200.
[38] J. Braegelmann, D. E. AM, S. Akmal, J. Maier, C. Braegelmann, J. Wenzel. *Acta Derm Venereol.* **2016**, *96*, 386.
[39] A. M. D'Erme, D. Wilsmann-Theis, J. Wagenpfeil, M. Holzel, S. Ferring-Schmitt, S. Sternberg, M. Wittmann, B. Peters, A. Bosio, T. Bieber, J. Wenzel. *J Invest Dermatol.* **2015**, *135*, 1025.
[40] A. Johnston, X. Xing, A. M. Guzman, M. Riblett, C. M. Loyd, N. L. Ward, C. Wohn, E. P. Prens, F. Wang, L. E. Maier, S. Kang, J. J. Voorhees, J. T. Elder, J. E. Gudjonsson. *J Immunol.* **2011**, *186*, 2613.
[41] M. Keermann, S. Koks, E. Reimann, E. Prans, K. Abram, K. Kingo. *BMC Genomics.* **2015**, *16*, 322.
[42] S. Hessam, M. Sand, T. Gambichler, M. Skrygan, I. Ruddel, F. G. Bechara. *Br J Dermatol.* **2018**, *178*, 761.

[43] K. Furue, T. Ito, Y. Tanaka, A. Yumine, A. Hashimoto-Hachiya, M. Takemura, M. Murata, K. Yamamura, G. Tsuji, M. Furue. *J Dermatol Sci.* **2019**, *94*, 244.
[44] S. Otobe, M. Sugaya, R. Nakajima, T. Oka, N. Takahashi, M. Kabasawa, T. Miyagaki, Y. Asano, S. Sato. *J Dermatol.* **2018**, *45*, 468.
[45] H. Bachelez, S. E. Choon, S. Marrakchi, A. D. Burden, T. F. Tsai, A. Morita, H. Turki, D. B. Hall, M. Shear, P. Baum, S. J. Padula, C. Thoma. *N Engl J Med.* **2019**, *380*, 981.
[46] L. Wang, Y. Quan, Y. Yue, X. Heng, F. Che. *Oncol Lett.* **2018**, *15*, 4711.
[47] J. Lachner, V. Mlitz, E. Tschachler, L. Eckhart. *Sci Rep.* **2017**, *7*, 17446.
[48] S. Li, J. Amo-Aparicio, C. P. Neff, I. W. Tengesdal, T. Azam, B. E. Palmer, R. Lopez-Vales, P. Bufler, C. A. Dinarello. *Proc Natl Acad Sci U S A.* **2019**.
[49] C. A. Dinarello, C. Nold-Petry, M. Nold, M. Fujita, S. Li, S. Kim, P. Bufler. *Eur J Immunol.* **2016**, *46*, 1067.
[50] M. F. Nold, C. A. Nold-Petry, J. A. Zepp, B. E. Palmer, P. Bufler, C. A. Dinarello. *Nat Immunol.* **2010**, *11*, 1014.
[51] R. Glaser, F. Navid, W. Schuller, C. Jantschitsch, J. Harder, J. M. Schroder, A. Schwarz, T. Schwarz. *J Allergy Clin Immunol.* **2009**, *123*, 1117.
[52] M. Kennedy Crispin, J. Fuentes-Duculan, N. Gulati, L. M. Johnson-Huang, T. Lentini, M. Sullivan-Whalen, P. Gilleaudeau, I. Cueto, M. Suárez-Fariñas, M. A. Lowes, J. G. Krueger. *Journal of Investigative Dermatology.* **2013**, *133*, 692.
[53] J. Nousbeck, A. Ishida-Yamamoto, M. Bidder, D. Fuchs, K. Eckl, H. C. Hennies, N. Sagiv, A. Gat, M. Gini, I. Filip, H. Matz, I. Goldberg, C. D. Enk, O. Sarig, B. Meilik, D. Aberdam, A. Gilhar, E. Sprecher. *J Invest Dermatol.* **2011**, *131*, 1767.
[54] K. Konig, L. Marth, J. Roissant, T. Granja, C. Jennewein, V. Devanathan, M. Schneider, D. Kohler, A. Zarbock, P. Rosenberger. *Eur J Immunol.* **2014**, *44*, 2648.
[55] G. Ertugrul, D. Keles, G. Oktay, S. Aktan. *Archives of Dermatological Research.* **2018**, *310*, 173.
[56] L. Hao, G. Zhu, Y. Lu, M. Wang, J. Jules, X. Zhou, W. Chen. *FEBS Lett.* **2015**, *589*, 1331.
[57] F. Jiang, Y. Gao, C. Dong, S. Xiong. *Biochem Biophys Res Commun.* **2018**, *504*, 734.

TABLE 1: Differentially expressed genes (DEGs)

Gene symbol	Gene	Fold change	FDR-adj P-value	Avg Exp Untreated (log 2)	Avg Exp UVB x 3 (log 2)
IL37	interleukin 37	4.54	0.016	7.8	9.98
MLANA	melan-A	4.04	0.001	10.9	12.91
LOR	loricrin	3.87	0.007	13.26	15.22
IGFBP7	insulin like growth factor bind protein 7	3.35	< 0.001	12.5	14.25
PMEL	premelanosome protein	3.21	0.001	8.09	9.77
KRT15	keratin 15, type I	3.07	0.001	11.99	13.61
TYRP1	tyrosinase-related protein 1	2.97	0.002	14.58	16.15
PLP1	proteolipid protein 1	2.96	0.001	9	10.56
TMEM99	transmembrane protein 99	2.9	0.004	6.32	7.86
PCSK2	proprotein convertase subtilisin	2.86	0.002	8.26	9.78
TYR	Tyrosinase	2.64	0.002	7.62	9.02
C5orf46	chromosome 5 open reading frame 46	2.56	0.031	5.86	7.21
CTSK	cathepsin K	2.55	0.003	11.31	12.66
DCT	dopachrome tautomerase	2.55	0.016	13.4	14.75
CAPN3	calpain 3	2.52	0.002	9.29	10.62
SAT1	spermine N1-acetyltransferase 1	2.47	< 0.001	9.84	11.14
KIT	v-kit sarcoma viral oncogene homolog	2.44	0.001	9.9	11.19
SERPINB12	serpin peptidase inh, clade B, member 12	2.42	0.005	12.75	14.03
LCE1D	late cornified envelope 1D	2.39	0.014	10.52	11.77
A2M	alpha-2-macroglobulin	2.38	0.007	8.05	9.3
CTSH	cathepsin H	2.35	0.001	8.23	9.47
AZGP1	alpha-2-glycoprotein 1, zinc-binding	2.35	0.003	12.16	13.39
TRPM1	transient rec potential cation channel M1	2.33	0.001	6.79	8.01
PLPPR4	phospholipid phosphatase related 4	2.3	< 0.001	6.04	7.24
CLU	Clusterin	2.29	0.026	7.63	8.83

ENPP2	ectonucleotide pyrophosphatase 2	2.24	< 0.001	8.51	9.68
SERPINF1	serpin peptidase inhibitor, clade F, M1	2.22	0.024	10.09	11.24
PLXNC1	plexin C1	2.22	0.002	8.22	9.37
SPARCL1	SPARC like 1	2.21	0.003	11.61	12.76
PLXDC1	plexin domain containing 1	2.17	0.020	8.4	9.52
KITLG	KIT ligand	2.16	0.003	8.28	9.39
MXRA5	matrix-remodelling associated 5	2.13	0.001	9.91	10.99
LCE1A	late cornified envelope 1A	2.12	0.031	9.85	10.93
LCE1B	late cornified envelope 1B	2.11	0.023	8.37	9.45
MMP2	matrix metallopeptidase 2	2.11	0.038	12.36	13.43
FTL	ferritin, light polypeptide	2.1	0.001	12.32	13.39
AKAP12	A kinase (PRKA) anchor protein 12	2.09	0.009	6.01	7.07
ABCA1	ATP binding cassette subfamily A1	2.08	< 0.001	9.5	10.56
TXNIP	thioredoxin interacting protein	2.06	0.003	11.98	13.02
FLG2	filaggrin family member 2	2.05	0.007	16.47	17.51
VIM	Vimentin	2.05	0.002	12.35	13.38
PTPRM	protein tyrosine phosphatase, RT M	2.03	< 0.001	9.3	10.32
FCGR3B	Fc fragment of IgG, low affinity IIIb	2.02	0.007	4.38	5.39
NPL	N-acetylneuraminate pyruvate lyase	2.01	0.002	6.55	7.55
FMN1	formin 1	2.01	0.001	8.31	9.31
WDR63	WD repeat domain 63	2	0.006	5.58	6.59
ASPA	Aspartoacylase	2	0.013	6.69	7.69
ENDOU	endonuclease, polyU-specific	-2	0.006	8.52	7.52
IL36A	interleukin 36, alpha	-2.01	0.001	4.5	3.5
KLK10	kallikrein related peptidase 10	-2.03	0.025	8.33	7.31
EREG	Epiregulin	-2.04	0.016	8.6	7.58
KLK9	kallikrein related peptidase 9	-2.05	0.015	8.09	7.05

GPATCH4	G-patch domain containing 4	-2.09	0.020	8.87	7.81
SQLE	squalene epoxidase	-2.12	0.004	11.91	10.83
DHRS9	dehydrogenase/reductase (SDR family) 9	-2.13	0.020	6.62	5.53
ME1	malic enzyme 1, $NADP^+$-dependent	-2.18	0.041	11.4	10.27
TMEM45B	transmembrane protein 45B	-2.27	0.012	13.42	12.24
FOSL1	FOS-like antigen 1	-2.39	0.049	6.49	5.24
SLC5A1	solute carrier family 5, member 1	-2.41	0.006	10.41	9.14
PLA2G2F	phospholipase A2, group IIF	-2.61	0.0201	10.34	8.95
PRSS22	protease, serine, 22	-2.77	0.003	8.22	6.75
PRSS3	protease, serine, 3	-2.83	0.003	10.22	8.71
S100A12	S100 calcium binding protein A12	-2.87	0.025	7.11	5.59
S100A7A	S100 calcium binding protein A7A	-3.11	0.043	15.26	13.63
SPRR2F	small proline-rich protein 2F	-3.13	0.002	8.98	7.33
IL36G	interleukin 36, gamma	-3.24	0.001	10.7	9
DEFB103A	defensin, beta 103A	-3.34	0.003	9.96	8.22
DEFB103AB	defensin, beta 103A; defensin, beta 103B	-3.48	0.004	9.68	7.88
SPRR2D	small proline-rich protein 2D	-3.5	0.025	15.9	14.09
SPRR2B	small proline-rich protein 2B	-3.76	0.016	15.05	13.14
FGFBP1	fibroblast growth factor binding protein 1	-3.76	0.013	9.75	7.83
ODC1	ornithine decarboxylase 1	-4.15	< 0.001	11.22	9.16
LCE3A	late cornified envelope 3A	-4.28	0.001	9.2	7.1
DEFB4A	defensin, beta 4A	-5.21	0.001	8.32	5.94
DEFB4B	defensin, beta 4B	-5.62	0.001	7.27	4.78
SPRR2A	small proline-rich protein 2A	-7.18	0.012	15.93	13.09
HEPHL1	hephaestin-like 1	-7.53	0.005	10.77	7.86

Figure legends

FIGURE 1: Experimental design and clinical scorings

One active lesion of eczema was biopsied before local irradiation with 1 MED nb-UVB on day 0, 2 and 4 and new biopsies were taken on day 7. The patients then underwent full body treatment with nb-UVB three times a week for 6-8 weeks, followed by another biopsy. All biopsies were bisected and stored for RNA isolation and for immunohistochemistry (a). Clinical scorings were performed before treatment (n = 16), after local nb-UVB times three (n = 16) and after 6-8 weeks of full body treatment (n = 15). Panels show SCORAD (b), EASI (c), POEM (d) and DQLI (e).

FIGURE 2: Local treatment with nb-UVB x 3 reveals little attenuation of epidermal hyperplasia nor leukocyte infiltration

Immunohistochemical stainings before (left column), after local nb-UVB treatment x 3 (middle column) and after 6-8 weeks of full body nb-UVB treatment (right column). Hematoxylin and eosin (a-c), Keratin 16 (brown) (d-f), $CD3^+$ cells (yellow), $CD4^+$ cells (purple), $CD8^+$ cells (teal), $FoxP3^+$ cells (brown). Most of the $CD3^+$-cells coexpress either $CD4^+$ (purple) to become orange, or $CD8^+$ (teal) to become green as the colors mix: $CD3^+/CD4^+$ cells (orange, arrows), $CD3^+/CD8^+$ cells (green, asteriks) (g-l), $CD11^+$ cells (teal) and $Langerin^+$ cells (purple) (m-r). J-l and p-r are enlargements of the smaller rectangle from the staining above. Scale bars 100μm.

FIGURE 3: Gene expression analysis.

Number of differentially expressed genes in lesional skin (LS) and non-lesional skin (non-LS) before and after treatment (a). PCA-plot showing gene expression from lesional skin from the same eczematous lesion at three different time points: untreated (blue dots, n = 16), after three treatments (red dots, n = 16) and after full-body treatment (purple dots, n = 14) (b). Gene

Ontology Analysis by Panther of the same genes: upregulated genes (c), downregulated genes (d). Volcano plot of the differentially expressed genes after only three treatments with nb-UVB (e).

FIGURE 4: IL-36γ and IL-37 are inversely regulated early after nb-UVB.

qRT-PCR showing downregulation of IL36γ and upregulation of IL37 after local nb-UVB x 3 (a). Immunohistochemistry confirms downregulation of IL36γ at the protein level. IL36γ green. Scale bars 50μm (b). The signal intensity is quantified, and the difference is significant (c).

FIGURE 1 Experimental design and clinical scorings

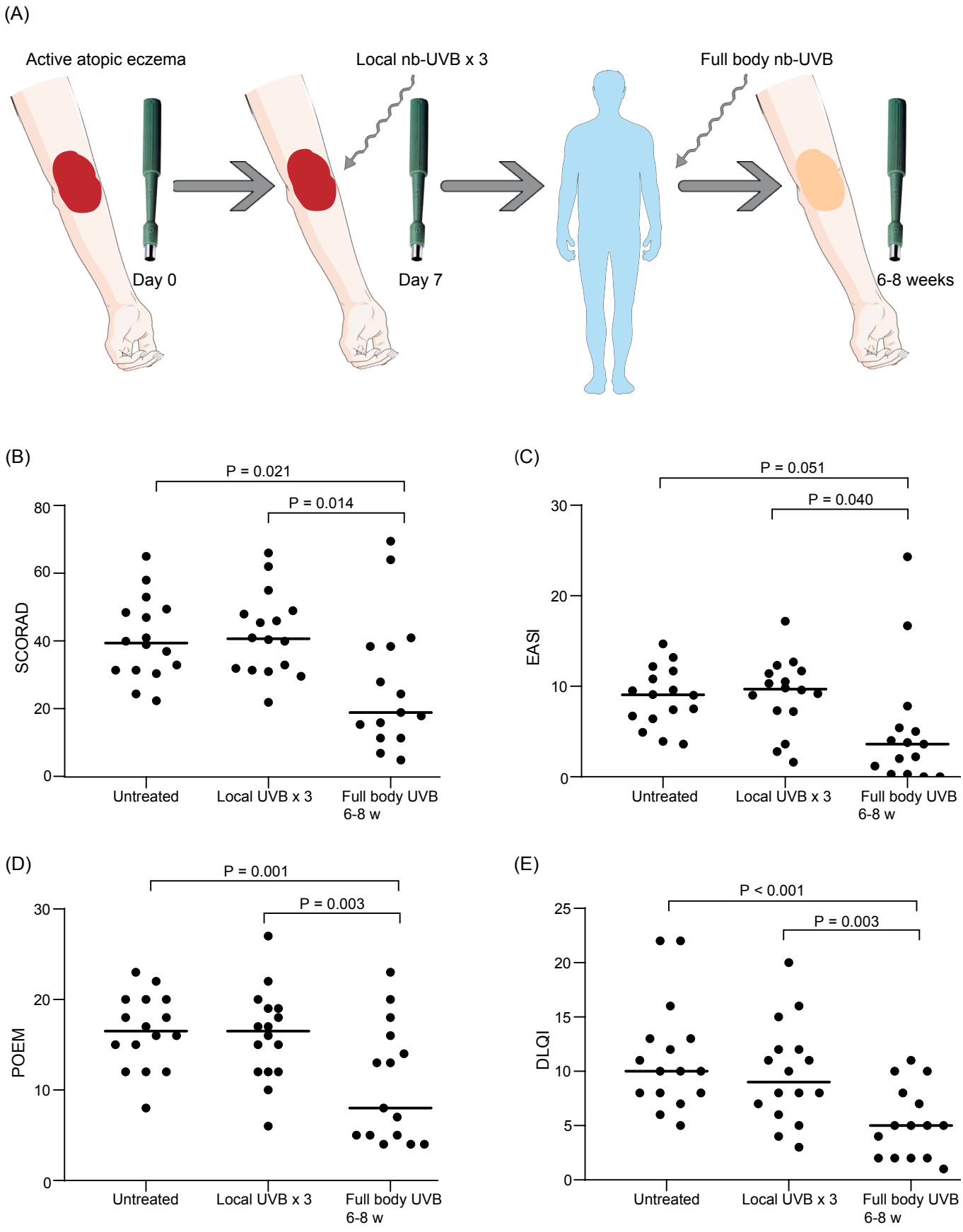

FIGURE 2 Local treatment with nb-UVB x 3 reveals little attenuation of epidermal hyperplasia nor leukocyte infiltration

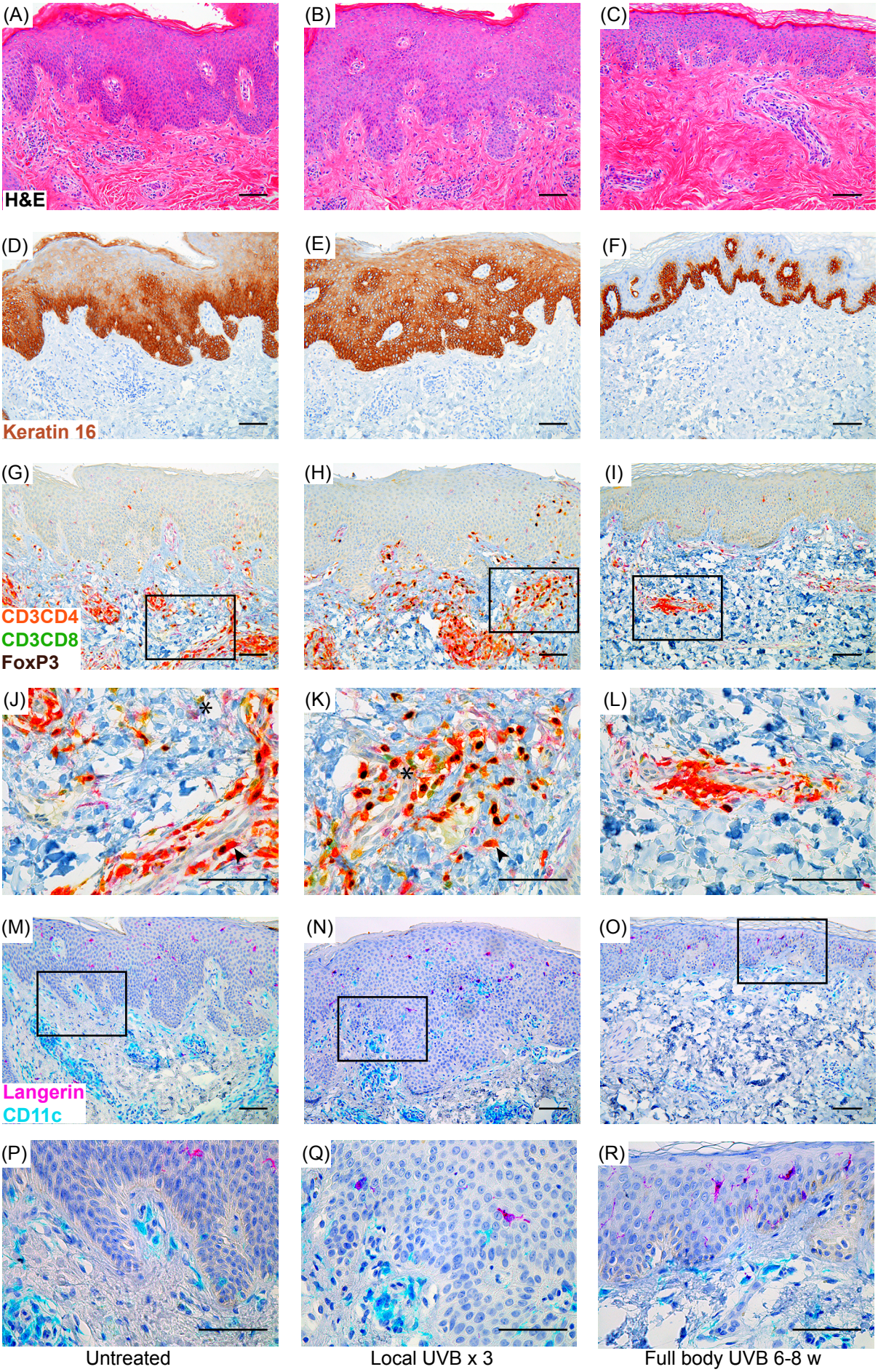

FIGURE 3 Gene expression analysis

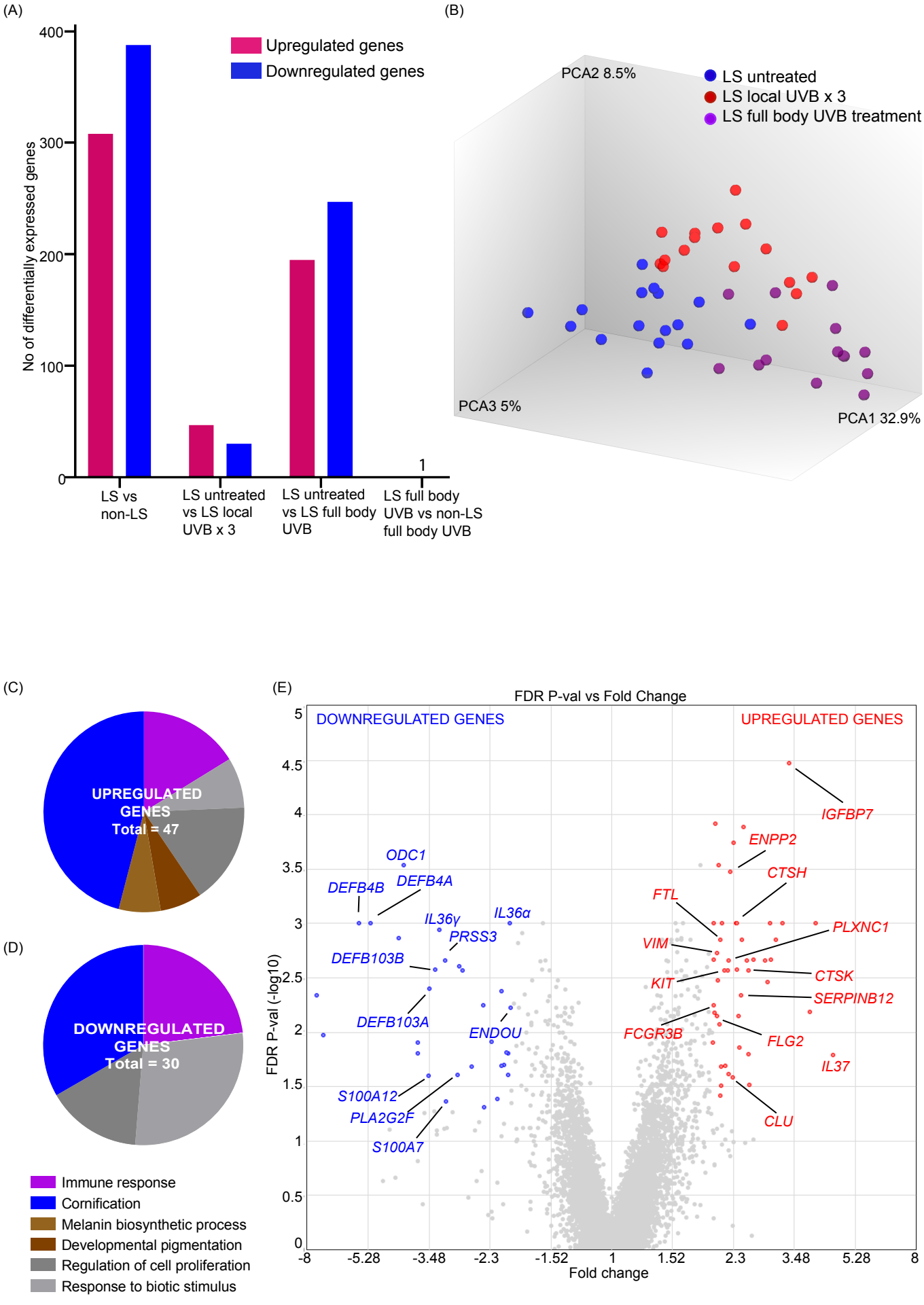

FIGURE 4 IL-36γ and IL-37 are inversely regulated early after nb-UVB

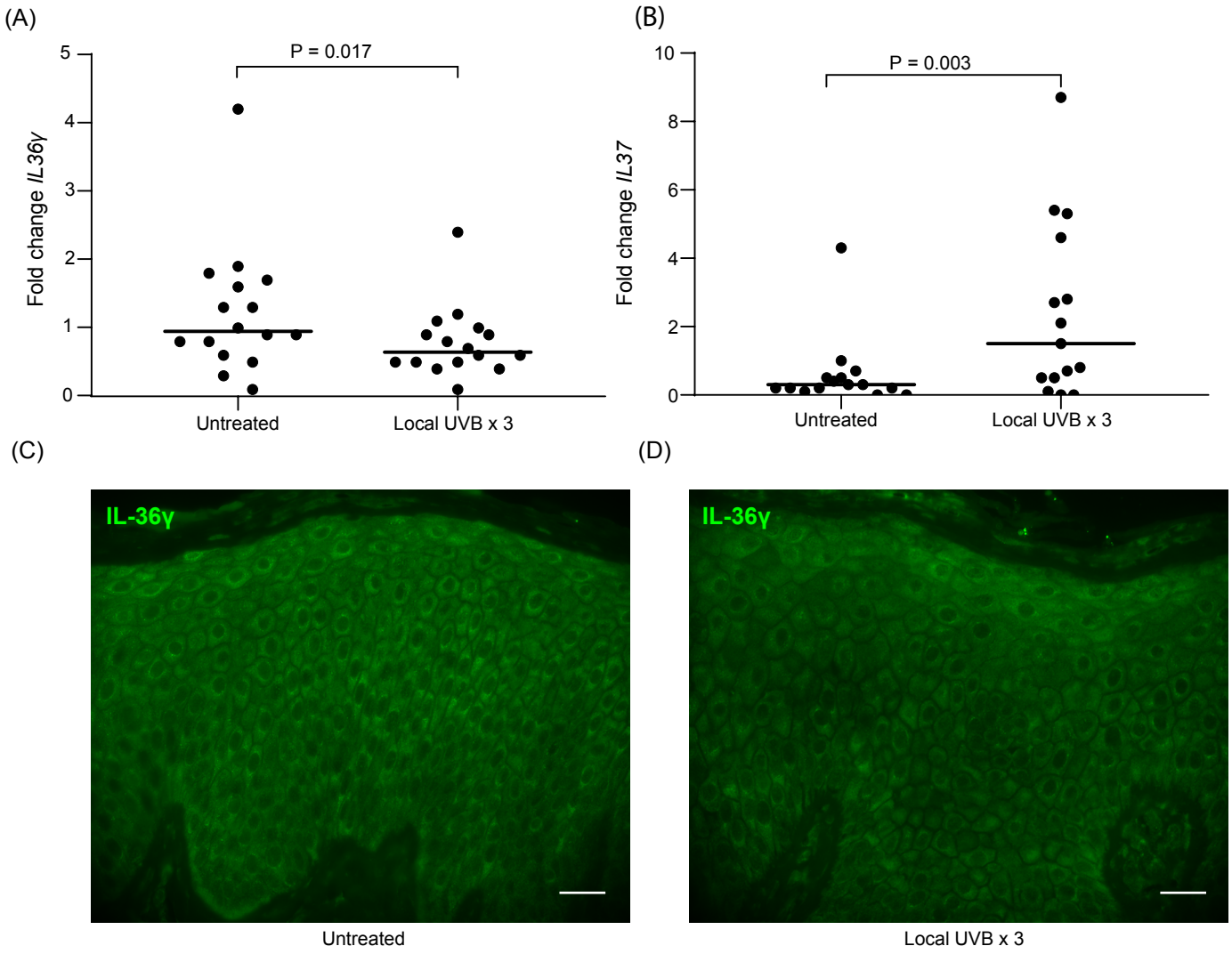

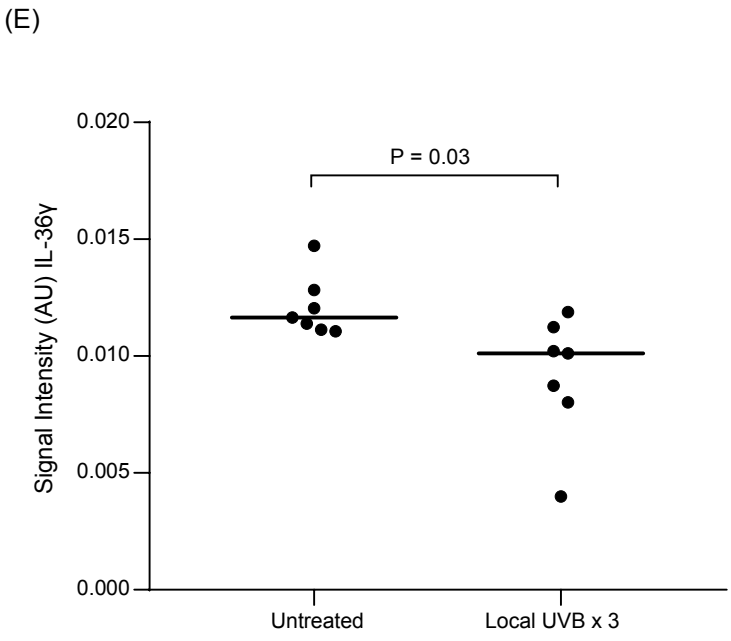

FIGURE S1

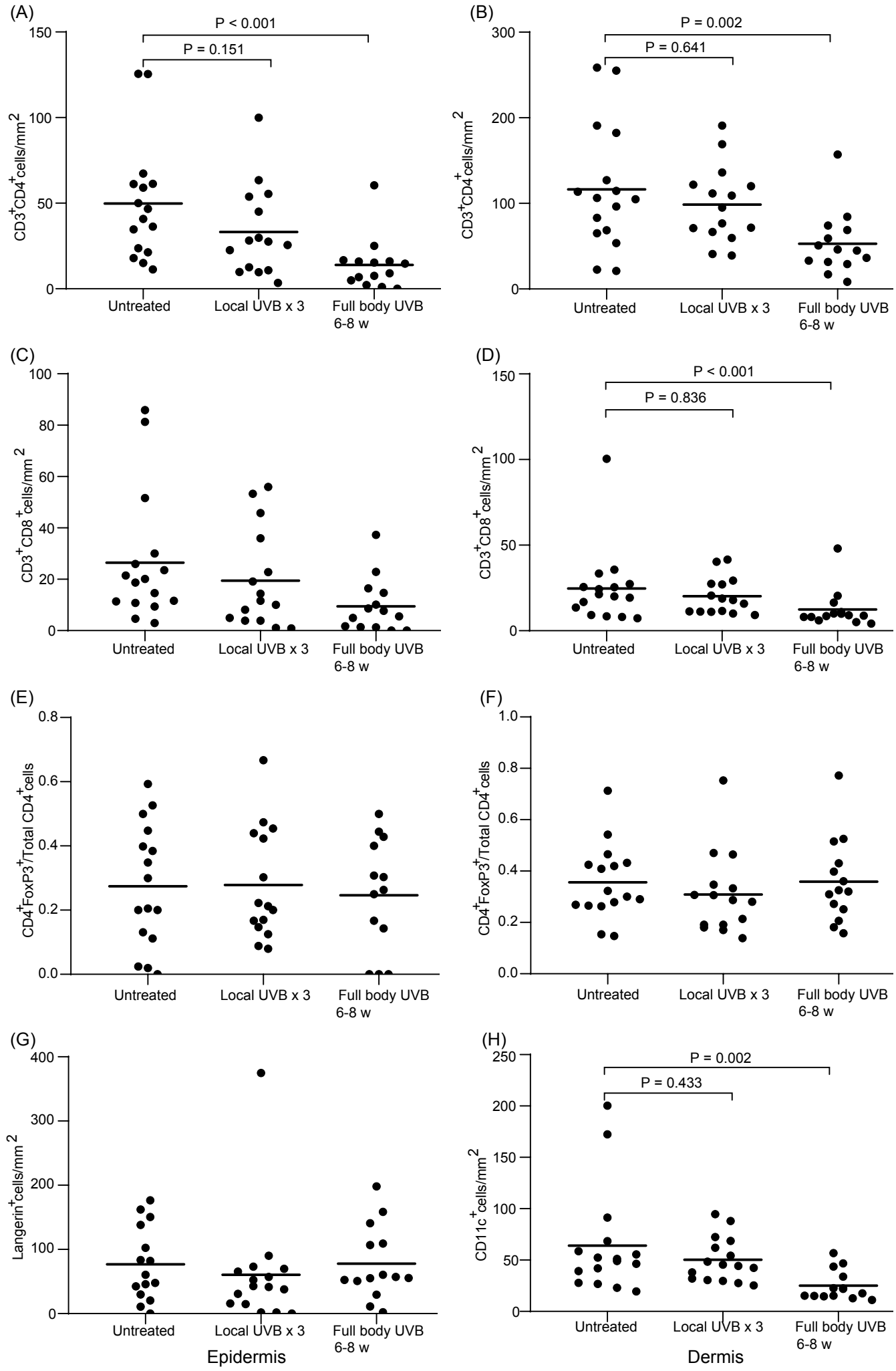
(A)
P < 0.001
P = 0.151
CD3+CD4+cells/mm2
Untreated
Local UVB x 3
Full body UVB 6-8 w
(B)
P = 0.002
P = 0.641
CD3+CD4+cells/mm2
Untreated
Local UVB x 3
Full body UVB 6-8 w
(C)
CD3+CD8+cells/mm2
Untreated
Local UVB x 3
Full body UVB 6-8 w
(D)
P < 0.001
P = 0.836
CD3+CD8+cells/mm2
Untreated
Local UVB x 3
Full body UVB 6-8 w
(E)
CD4+FoxP3+/Total CD4+cells
Untreated
Local UVB x 3
Full body UVB 6-8 w
(F)
CD4+FoxP3+/Total CD4+cells
Untreated
Local UVB x 3
Full body UVB 6-8 w
(G)
Langerin+cells/mm2
Untreated
Local UVB x 3
Full body UVB 6-8 w
Epidermis
(H)
P = 0.002
P = 0.433
CD11c+cells/mm2
Untreated
Local UVB x 3
Full body UVB 6-8 w
Dermis

FIGURE S2

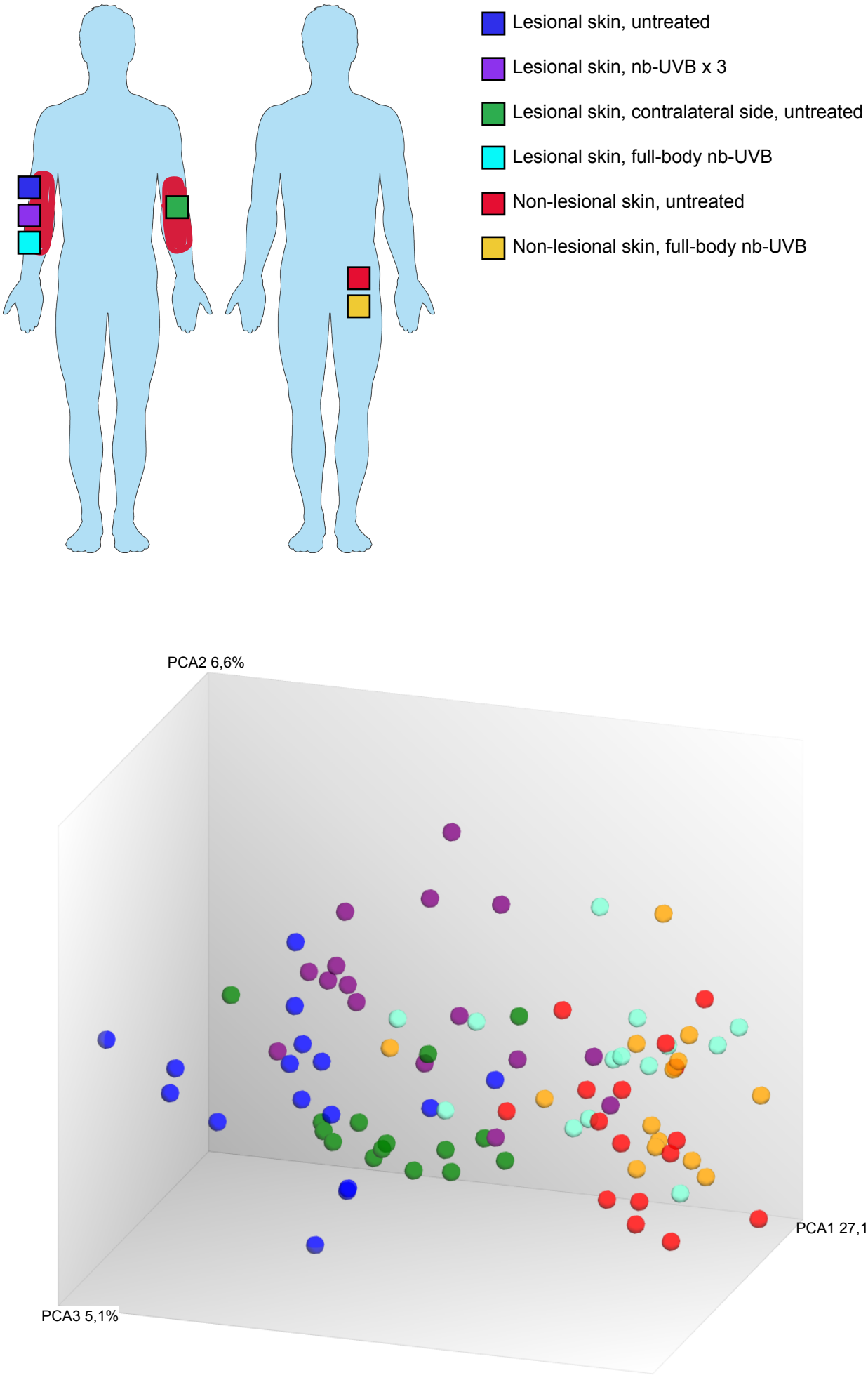
Lesional skin, untreated
Lesional skin, nb-UVB x 3
Lesional skin, contralateral side, untreated
Lesional skin, full-body nb-UVB
Non-lesional skin, untreated
Non-lesional skin, full-body nb-UVB
PCA2 6,6%
PCA1 27,1%
PCA3 5,1%

FIGURE S3

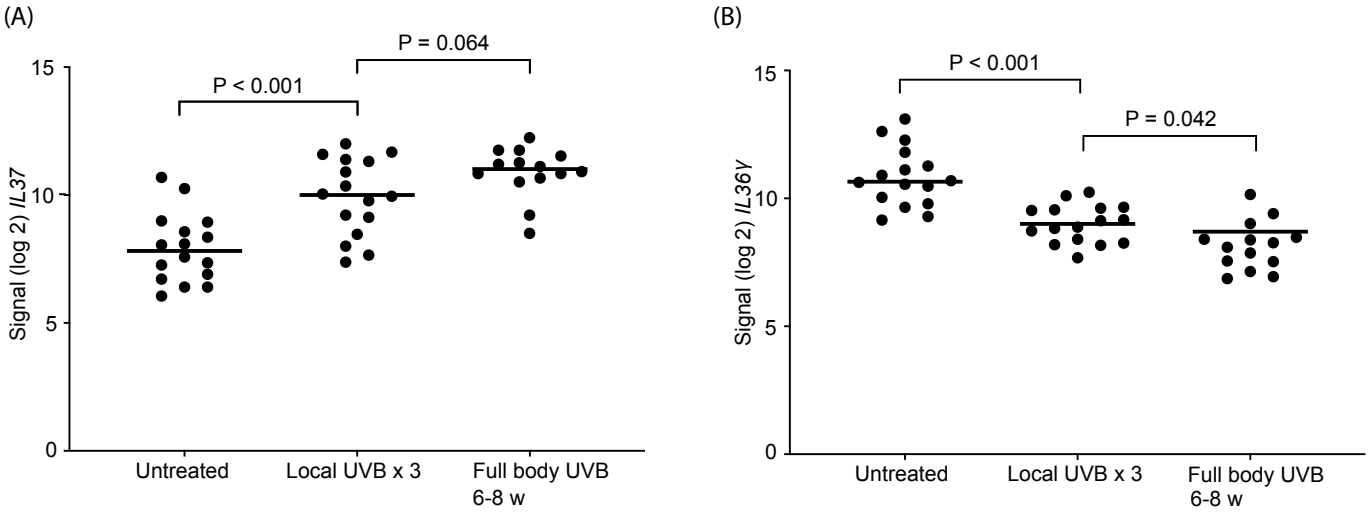
(A)
P = 0.064
P < 0.001
15
10
5
0
Signal (log 2) IL37
Untreated
Local UVB x 3
Full body UVB
6-8 w
(B)
P < 0.001
P = 0.042
15
10
5
0
Signal (log 2) IL36Y
Untreated
Local UVB x 3
Full body UVB
6-8 w